SAND2017-6806J

Paper

REASSESSMENT OF RESUSPENSION FACTOR FOLLOWING RADIONUCLIDE DISPERSAL: TOWARDS A GENERAL-PURPOSE RATE CONSTANT

Shaun Marshall*, Charles Potter†, and David Medich*

***Abstract* — A recent analysis of historical radionuclide resuspension datasets confirmed the general applicability of the Anspaugh and modified Anspaugh models of resuspension factors following both controlled and disastrous releases. The observations appear to increase in variance earlier in time, however all points were equally weighted in statistical fit calculations, inducing a positive skewing of resuspension coefficients. Such data are extracted from the available deposition experiments spanning 2900 days. Measurements within a 3-day window are grouped into singular sample sets to construct standard deviations. A refitting is performed using a relative instrumental weighting of the observations. The resulting best-fit equations produces tamer exponentials which give decreased integrated resuspension factor values relative to those reported by Anspaugh. As expected, the fits attenuate greater error amongst the data at earlier time. The reevaluation provides a sharper contrast between the empirical models, and reaffirms their deficiencies in the short-lived timeframe wherein the dynamics of particulate dispersion dominate the resuspension process.**

Key words: dispersion, radiological; resuspension factor; contamination, environmental

INTRODUCTION

Evaluating prospective dose for emergency planning and response, health physics operations, or setting of thresholds for radiological security, has become an important part of health physics. When the dose to be considered is primarily internal, the exposure profile and associated characteristics are vital to an appropriate estimate. This includes physical and chemical properties of the element in question that would define the amount of dispersed material that has become airborne or resuspension. Particular elements may react physically or chemically with substrates preventing such action or radiological properties such as aggregate recoil may come into play. Allen Brodsky's famous note from 1979 started the discussion of 10^{-6} m^2/m^3 being a value that could be used conservatively in the absence of a better value.Brodsky (1980)

Resuspension models have been developed for use in such prospective dose evaluations using data from existing studies. Measurements have been taken for estimation of resuspension, whether opportunistic or as a result of specific experimental design. The nominal reference for resuspension is NCRP Report 129.(NCRP, 1999) A more recent review and analysis in support of the Federal Radiological Monitoring and Assessment Center (FRMAC) was conducted by Maxwell and Anspaugh in 2011 the results of which are currently being used by the FRMAC community.(Maxwell and Anspaugh, 2011) A review of the available data and methodologies resulted in a desire to determine if resuspension properties including chemical interactions with surface materials and particle size of resuspended material could be determined to develop a more holistic model that would apply to a particular radionuclide. Americium-241, being a current radionuclide of interest, was chosen for this study. This work begins with a review and reassessment of previous work. A future paper or papers will describe the experimental process and results.

I. Internal Dosimetry of Inhaled Radionuclides

FRMAC publishes an assessment manual for determining action limits in the event of a radiological incident. This limit is represented by dose response levels (DRLs) which are in agreement with the Protective Action Guide developed by the US Environmental Protection Agency (EPA) and the Department of Homeland Security (DHS). In calculating this limit, exposure pathways are considered separately then combined, including the deposition inhalation dose parameter $Dp\_InhDpDC$ $(mrem)$ from inhaling resuspended radionuclides from a contaminated area (Eq. 1):

$$Dp\_InhDpDC_{i,TP} = InhDC_i \cdot KP_{i,TP} \cdot BR_{AA}, \quad (1)$$

- $InhDC_i$ is the inhalation committed dose coefficient for radionuclide i $(mrem/Ci)$,
- BR_{AA} is the activity-averaged human breating rate (usually taken as 0.92 m^3/h)
- $KP_{i,TP}$ is the resuspension parameter $(Ci \cdot s/m^3)$, which considers airborne concentration of radionuclide i during the given time phase, with radioactive decay/in-growth and resuspension factor K_t (Eq. 2):

$$KP_{i,TP} = \int_{t_1}^{t_2} K_t \cdot Dp_{i,t_0} \cdot e^{-\lambda_i t}, \quad (2)$$

- Dp_{i,t_0} is the initial deposition of radionuclide i

*Department of Physics, Worcester Polytechnic Institute, Worcester, MA
†Sandia National Laboratories, Albuquerque, NM
The authors declare no conflicts of interest.
For correspondence contact: S. Marshall at shaun@wpi.edu.

- λ_i is the decay coefficient of radionuclide i
- K_t is the empirical resuspension factor as reported by Maxwell and Anspaugh (2011) (Eq. 3):

$$K_t = \left(10^{-5}\right) e^{-(8.1\cdot 10^{-7})t} + \left(7\cdot 10^{-9}\right) e^{-(2.31\cdot 10^{-8})t} + 10^{-9}. \quad (3)$$

The resuspension factor K_t (m^{-1}) is computed by dividing the air activity concentration (Ci/m^3) by the areal activity of the deposition (Ci/m^2). Literature demands data collection to be taken under calm, isolated conditions. Antropological mechanical disturbances, including the induced turbulance from the walking of a passer-by, have been to produce resuspenion levels of 10^{-10} to 10^{-2} (Langham, 1971).

II. Atmospheric resuspension and deposition rates, particle size distributions

Particulates bound to the ground surface layer are stochastically resuspended in the presence of turbulent air currents; the resuspension rate increases with boundary layer lateral air velocity (Chkhetiani et al., 2012). An analytical foundation of the kinetic "desorption" rate constant from a surface begins with Reeks et al (1988), in which the total aerodynamic lift force exceeds the total adhesion force. The fraction removed f_R and resuspension rate Λ (s^{-1}) for identical *smooth* sites follow a simple Arrhenius law (Eq. 4):

$$f_R(t) = e^{-k_{sus}t}, \qquad \Lambda(t) = -\dot{f_R} = k_{sus}e^{-k_{sus}t} \quad (4)$$

Even the updraft caused by the the air sampler induces an additional resusupending force on the surface particles, which populates the air concentration beyond the "true background" resuspension from Brownian atmospheric fluctuations. Practically, this accoustic intrusion is reciprocated by the individual's own inhalation at the same flowrate in the vicinity, though with more unique nozzle and air inlet boundaries and in/outflow rates, so particulate collection on the personal air sampler filters are applicable. Still, a non-circulating sampling method within a closed system would enable measurement of the "true background" resuspension in equilibrium with the other compartments.

The resuspended particle size distribution evolves from that of the initial surface deposition (Anspaugh et al., 2002). Fine particulates have been found to make up a significant portion of resuspended material under light wind conditions (Chkhetiani et al., 2012), but coarse particulates increase in presence with lateral wind speed (Henry and Minier, 2014). A *roughness* surface rate constant can serve as the functional preference for particle size (Ziskind et al., 1995). The standard treatment is Gaussian potential barrier which is lowest at a preferred size r^*; deviation for a particle r_a will lower the rate constant as Eq. 5:

$$k_{sus}(r_a) = \frac{\omega_0}{2\pi} e^{-\frac{(r_a - r^*)^2}{r_0^2}}, \quad (5)$$

where r_0 characterizes the sensitivity of the deviation effect and $\frac{\omega_0}{2\pi}$ is the normalized maximum rate constant. In practice ω_0 is a function of wind speed which acoustically resonates with characteristic particle sizes; full derivations of this "rock n' roll" algorithm can be found in a recent paper by Caruso (2015) probing dust resuspension models. Resuspended particulates tend to be well-characterized by [activity] median aerodynamic diameter (AMD) and the geometric standard deviation (Liu et al., 2014).

IV. Ground sorption, migration, and mixing rates

Kinetic models for sorption and desorption of radionuclides to the surface binding sites at a boundary layer, and for colloid in the bulk ground matrix, have been employed successfully in both under- and oversaturated conditions (Lujaniene et al., 2012). Americium is readily absorbed into clays and organic mineral oxide topsoils (Bunzl et al., 1995; Lee and Lee, 2000). In colloidal form, Americium is strongly kinetic in granodiorite and infill (et al, 2003; Vilks and Bachinski, 1996), but shows preference for anionic sorption in cementous pastes (Evans, 2008). It had significantly decreased mobility in the presence of snow drifts/melts compared Alkali and Alkaline Earth metals (Chawla et al., 2010). Foliage in the region accumulates resuspended material proportionate to increased railfall intensity and frequency (Dreicer et al., 1984).

Bioturbiders, burrowing organisms which actively mix bulk material through digging or ingestion, may also contribute to radionuclide movement. Earthworms have been found to overturn 1 meter of topsoil with a throughput of 5-10 years (Muller-Lemens and van Dorp, 1996). This type of movement is difficult to model as a kinetic process, but is well-described by random diffusive mixing processes, with some models which estimate the coefficient to be ∼1-2 cm^2/year (Matisoff et al., 2011).

V. Resuspension Catenary Models

If particulates are laterally confined to move in a turbulent column of atmosphere, Eq. 4 can expanded with the deposition process, the inverse reaction to resuspension shown by the recycling kinetic formula (Eq. 6):

$$\boxed{A} \underset{k_{A\leftarrow S}}{\overset{k_{A\rightarrow S}}{\rightleftharpoons}} \boxed{S}, \quad (6)$$

where S is the catenary compartment tracking the particles bound to the surface, and A considers the particulates suspended in the air. The rate equations (Eq. 7) and proceeding general solutions solutions (Eq. 8) to this system are

$$\begin{cases} \dot{X_A} &= -k_{A\rightarrow S}X_A + k_{A\leftarrow S}X_S \\ \dot{X_S} &= k_{A\rightarrow S}X_A - k_{A\leftarrow S}X_S \end{cases}, \quad \text{and} \quad (7)$$

$$\begin{cases} X_A(t) &= X_{A,0} + X_{A,1}e^{-(k_{A\rightarrow S}+k_{A\leftarrow S})t} \\ X_S(t) &= X_{S,0} + X_{S,1}e^{-(k_{A\rightarrow S}+k_{A\leftarrow S})t} \end{cases}, \quad (8)$$

where doublets $X_{A,0}$, $X_{S,0}$ are the equilibrium concontrations, and $X_{A,1}$, $X_{S,1}$ are assigned based on initial conditions. The sign and magnitude of $X_{A,1}$ depends on whether the particulates are predominantly settling out or lifting off of the ground (airborne release or idealized surface deposition respectively. Using initial constraints $X_A(0)$ and $X_S(0)$, unique solutions are found (Eq. 9).

$$\begin{cases} X_{A,0} &= \left[\dfrac{X_A(0) - X_S(0)}{1 - \frac{k_{A\to S}}{k_{A\leftarrow S}}}\right] \\ X_{S,0} &= \left[\dfrac{k_{A\to S}X_A(0)}{k_{A\leftarrow S} - k_{A\to S}}\right] \\ X_{A,1} &= X_{S,1} = \left[\dfrac{k_{A\leftarrow S}X_S(0) - k_{A\to S}X_A(0)}{k_{A\leftarrow S} - k_{A\to S}}\right] \end{cases} \tag{9}$$

Over longer periods of time the contribution of ground layer migration may become appreciable, and thus require its own kinetic form with mixing/"convection" reverse reactions to bring particles from the ground bulk matrix G to the surface (Eq. 10):

$$\boxed{A} \underset{k_{A\leftarrow S}}{\overset{k_{A\to S}}{\rightleftharpoons}} \boxed{S} \underset{k_{S\leftarrow G}}{\overset{k_{S\to G}}{\rightleftharpoons}} \boxed{G}. \tag{10}$$

Realistically, this would continue into a fractal of ground bulk matrix pathways available to the radionuclide depending on the physicochemical properties of the nuclide and substrate. The solution is therefore an incomplete picture of the radionuclide movement, but nonetheless an accurate model for measurements shorter than geological timescales. The rate equations and solution (Eqs. 11, 12) to this resemble that of the two-comparment model (Eqs. 7, 8):

$$\begin{cases} \dot{X_A} &= -k_{A\to S}X_A \quad + \quad k_{A\leftarrow S}X_S \\ \dot{X_S} &= \quad k_{A\to S}X_A - (k_{A\leftarrow S} + k_{S\leftarrow G})X_S + k_{S\to G}X_G \\ \dot{X_G} &= \qquad\qquad k_{S\to G}X_S \; - \; k_{S\leftarrow G}X_G \end{cases}, \tag{11}$$

and

$$\begin{cases} X_A(t) &= X_{A,0} + X_{A,1}e^{\lambda_1 t} + X_{A,2}e^{\lambda_2 t} \\ X_S(t) &= X_{S,0} + X_{S,1}e^{\lambda_1 t} + X_{S,2}e^{\lambda_2 t} \\ X_G(t) &= X_{G,0} + X_{G,1}e^{\lambda_1 t} + X_{G,2}e^{\lambda_2 t} \end{cases}, \tag{12}$$

$$\text{with } \lambda_{1,2} = -\frac{1}{2}\left[B \mp \sqrt{B^2 - 4C}\right] \tag{13}$$

$$\text{where } B = k_{S\leftarrow G} + k_{A\to S} + k_{A\leftarrow S} + k_{S\to G},$$

$$\text{and } C = k_{A\to S}k_{S\to G} + k_{A\to S}k_{S\leftarrow G} + k_{A\leftarrow S}k_{S\leftarrow G},$$

and doublets $X_{A,0}$, $X_{A,1}$, $X_{S,0}$, $X_{S,1}$, and $X_{G,0}$, $X_{G,1}$ are assigned by initial conditions. The discriminant of the decay constants in Eq. 13 is positive, confirming an overdamped process. The system achieves equilibrium with the following conditions (Eq. 14):

$$X_{A,0} = \frac{k_{A\leftarrow S}}{k_{A\to S}}X_{S,0} = \frac{k_{A\leftarrow S}k_{S\leftarrow G}}{k_{A\to S}k_{S\to G}}X_{G,0}. \tag{14}$$

Following a non-ideal airborne release of particulates ($X_G(0) = 0$), the quantity available for air sampling decays exponentially over two processes characterized by timescales $\dfrac{1}{\lambda_2} < \dfrac{1}{\lambda_1}$. Using the remaining initial conditions $(X_A(0), X_S(0))$, the unique solution is generated for the air compartment (Eq. 15):

$$\begin{cases} X_{A,0} &= (X_A(0) + X_S(0))\,\dfrac{k_{A\leftarrow S}k_{S\leftarrow G}}{\lambda_1\lambda_2} \\ X_{A,1} &= \dfrac{\begin{array}{c} X_A(0)\left(\lambda_1^2 \; + \; \lambda_1(k_{S\to G} + k_{S\leftarrow G} + k_{A\leftarrow S})\right) \\ + \quad (X_A(0) + X_S(0))\,k_{A\leftarrow S}\,(k_{S\leftarrow G} + \lambda_1) \end{array}}{\lambda_1(\lambda_1 - \lambda_2)} \\ X_{A,2} &= \dfrac{\begin{array}{c} X_A(0)\left(\lambda_2^2 \; + \; \lambda_2(k_{S\to G} + k_{S\leftarrow G} + k_{A\leftarrow S})\right) \\ + \quad (X_A(0) + X_S(0))\,k_{A\leftarrow S}\,(k_{S\leftarrow G} + \lambda_2) \end{array}}{\lambda_2(\lambda_2 - \lambda_1)} \end{cases} \tag{15}$$

where $\lambda_{1,2}$ are defined in Eq. 13.

$X_A(t)$ intially possesses the entirety of the particulate release, which must gradually deposit onto the surface before resuspending. Depending upon the nature of the particulate release this condition may nearly exact, as in the case of stack emissions or active release mechanisms, or it may be skewed, in the case of spills or other passive releases. This variance is dependent upon the sampling conditions, which must be standardized to enable the discrete compartmentalization of surface (height $h = 0$ to -10 cm) and air (height $h = 1$ m). It is important to note that a sufficiently low resuspension rate constant $k_{A\leftarrow S}$ may lead to skewed interpretations on the quantity of particules which have undergone the resuspension mechanism at early timeframes.

The rate constants $(k_{S\leftarrow G}, k_{S\to G}, k_{A\to S}, k_{A\leftarrow S})$ and initial fractional values $X_A(0), X_S(0) = 1 - X_A(0)$ can be extracted from the values $X_{A,0}, X_{A,1}, X_{A,2}\lambda_1, \lambda_2$ (as from fitting coefficients) using a computational solver (in this work *Mathematica* was used). From these systematic parameters, limiting dispersion conditions of the ideal surface ($X_S(0) = 1$) or airborne ($X_A(0) = 1$) release may be probed.

METHODS

I. Historical Dataset of Resuspension Observations

Quantifying the internal dose of ionizing radiation from inhaled radionuclides is an inherently complex and event-specific problem. This is largely due to the high variability of the the factors which influence the resuspension of deposited particlates into the air, including aerosol size distribution (Karlsson et al., 1996), ambient temperature and pressure (Xu et al., 2016), humidity (Kim et al., 2016), vegetation and rainfall (Dreicer et al., 1984), and lateral wind speed (Harris and Davidson, 2008). During the non-nuclear Plutonium disperal tests of Project 56 at the Nevada Test Site (Langham et al., 1955), the resusupension factor S_f was developed as a metric to predict radiogenic risk from inhaled resuspended particulates. This broad-stroked ratio

of volumetric airborne radioactivity to that within a given area directly beneath requires detailed knowledge of the event conditions and site mechanical processes (Langham, 1971), but nonetheless remained successful in empirically identifying an nonlinear decay of suspended particulates over time post-dispersion (Garland, 1983; Tveten, 1990; Garland and Pomeroy, 1994). Attempts to optimize and evaluate functional models have predominantly leaned towards exponential behavior over polynomial or power-law (Garger et al., 1999). Recent difficulty in applying these sensitive approximations to early timeframes following deposition led to potentially 10-100x more conservative estimates (Maxwell and Anspaugh, 2011).

II. Observation Time-Binning and Statistics

Historic resuspension factor observations (Fig. 1) follows a heteroscedastic trend- the variance of proximate values can be seen to change (decrease) as a function of time. To enable statistical fitting of model, observations were first resolved as geometric averages within finite time-bins. Data were grouped into bins wide enough to encompass a local spread of coincidence; this was guided by habitual occurance of measurements within individual datasets. Statistics performed upon the binned values follow Eq. 16;

$$\mu_{S_f} = e^{\frac{1}{n}\sum^n \ln(S_f)}, \quad \sigma_{S_f} = e^{\sqrt{\frac{1}{n}\sum^n \left(\ln(S_f)-\mu_{S_f}\right)^2}} \tag{16}$$

III. Uncertainty-Weighted Fitting of Catenary Models

Bin averages were fit to a two-compartment cantenary model which can be extracted from the the particulate population in Eq. 12:

$$S_f(t) = X_{A,0} + X_{A,1}e^{\lambda_1 t} + X_{A,2}e^{\lambda_2 t}$$

using a linear least-squares regression. Y-data regression received an instrumental weighting bias $\left(w_i = \sigma_{Y_i}^{-2}\right)$, which serves to a) increase importance of low uncertainty coincidence present in long-term data and b) decrease importance of high uncertainty coincidence present in short-term data. The cantenary model was applied both with fixed 10^{-9} and unfixed offset constant, to test for greater compliance with newer data.

RESULTS

I. Resuspension Factor Observations

Resuspension data readily available from references of the assessment by Maxwell and Anspaugh (2011) were used. Some data, such as Tveten (1990) and Garger (1997) provided additional long-term observations than the sample depicted in the assessment which were also incorporated into this work. As few studies provided intrinsic collection error, uncertainty propagation was not included. Values are plotted in Fig. 1.

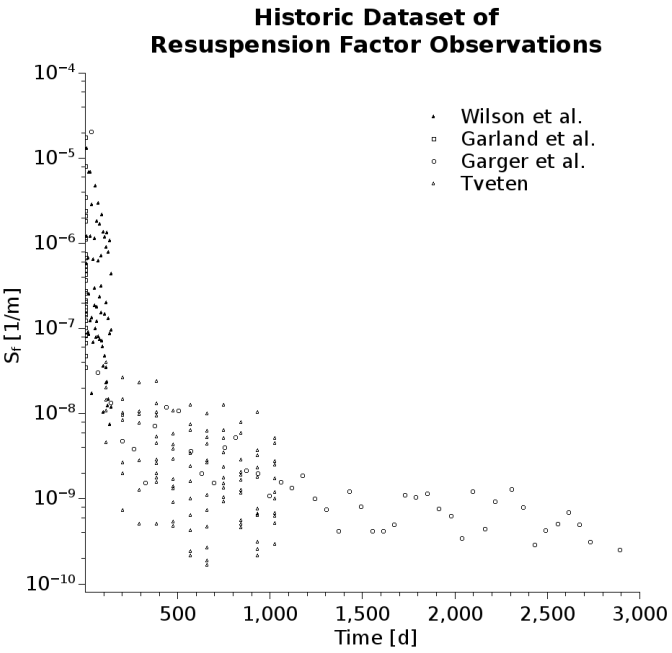

Figure 1: Semilog plot of resuspension factor observations from 0.005 to 2890 d.

II. Time-Binned Averages of Observations

Fig. 2 contains the historic dataset of resuspension observations binned into subsets with errorbars to designate geometric spread in days and resuspension factor. Bins with only one observation reused the lowest calculated spread from the remainder of the set to facilitate a *relative* instrumental weighting of each regression.

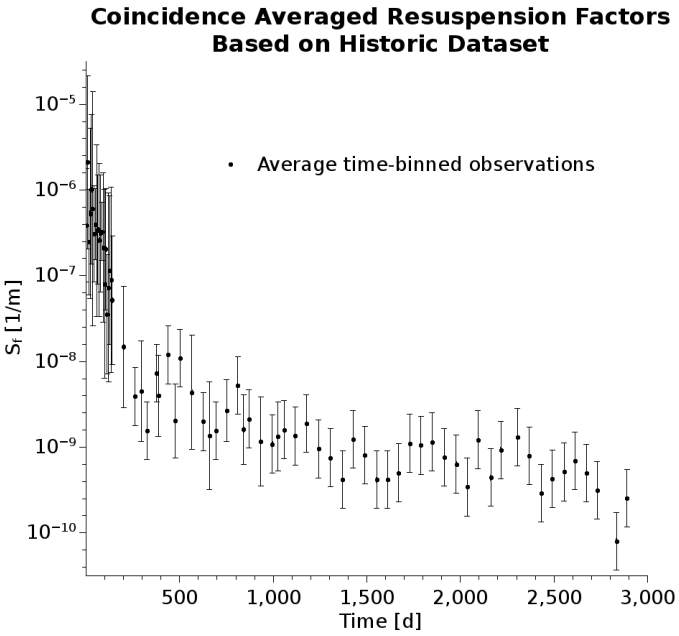

Figure 2: Semilog plot of time-bin averaged resuspension factor observations from 0.005 to 2890 d.

III. Catenary Model Weighted Fitting

Also rendered are plots of the regression for each model; parameters for each model obtained using Origin are given in Table 1. For better visibility of short-term processes, a log-log plot of these data and fits is provided in Fig. 3. Present in both this and Fig. 2 are constant lines drawn at $S_f = 10^{-9}$ to underscore the divergence between models prescribing this value of the functional offset and extended observations not before employed.

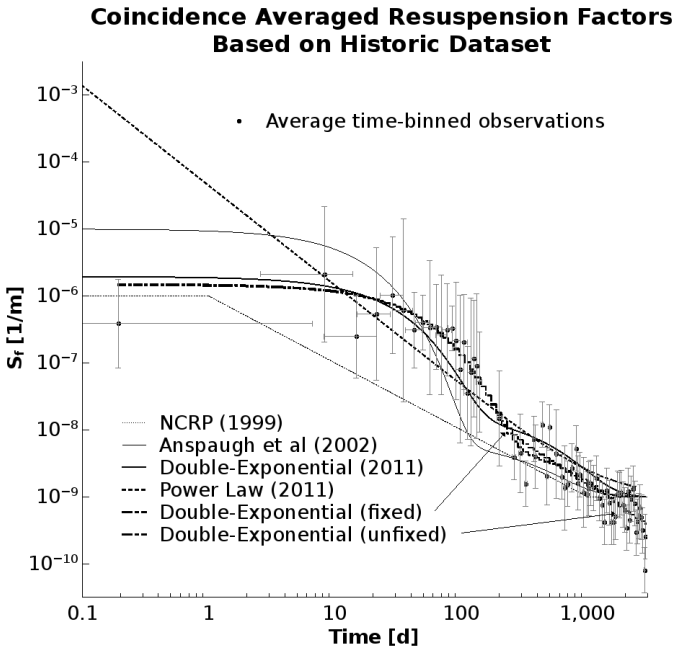

Figure 3: Log-log plot of averaged resuspension factor observations, overlayed with recent models including this work (indicated with arrows).

Table 1: Best-fit linear regression parameters in log-space of averaged observations with varied constant offset.

	fixed	unfixed
A_0	1.00×10^{-9}	3.307×10^{-10}
A_1	1.501×10^{-6}	1.450×10^{-6}
A_2	1.371×10^{-8}	6.118×10^{-9}
λ_1	-0.0264	-0.0253
λ_2	-0.00346	-0.00157

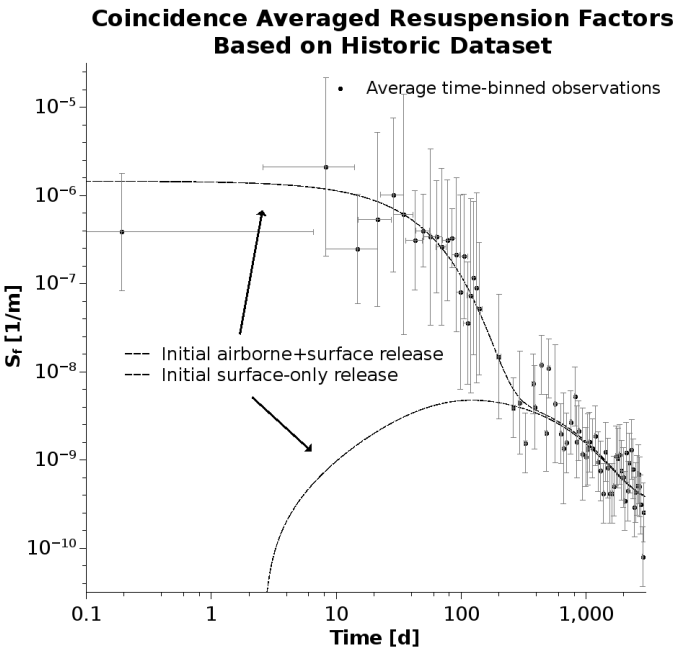

Figure 4: Log-log plot of averaged airborne to deposition ratio observations, overlayed with this works unfixed dual-exponential model and its corresponding limit of an ideal surface release $X_S(0)$.

Integrated resuspension factor (RF) values were calculated for the array of time periods following deposition used by Maxwell and Anspaugh (2011), and given in Table 2. Additionally, percent deviations in RF between the unfixed regression from this work and previous model predictions are given to illustrate the relative increase or decrease of this work's prediction of inhalation dose.

Table 2: Integrated resuspension factors for relative dose effect of regression models, values are in units of $d\ m^{-1}$. Also provided are over- (+) and underprediction (-) of this work's unfixed regression resuspension factor relative to each model at integral times.

	Integration period [days]				
	0-1	0-10	0-30	0-100	0-365
This work (fixed)	1.496×10^{-6}	1.334×10^{-5}	3.157×10^{-5}	5.454×10^{-5}	6.726×10^{-5}
This work (unfixed)	1.438×10^{-6}	1.288×10^{-5}	3.068×10^{-5}	5.344×10^{-5}	6.044×10^{-5}
This work, resuspension term (unfixed)	6.444×10^{-9}	6.401×10^{-8}	1.892×10^{-7}	5.993×10^{-7}	1.820×10^{-6}
NCRP Model	1.00×10^{-6}	3.30×10^{-6}	4.40×10^{-6}	5.61×10^{-6}	7.91×10^{-6}
(NCRP, 1999)	+43.8%	+290%	+597%	+849%	+666%
Double-Exponential	1.89×10^{-6}	1.60×10^{-5}	3.42×10^{-5}	4.86×10^{-5}	5.05×10^{-5}
(Maxwell and Anspaugh, 2011)	-24.0%	-19.5%	-10.3%	+9.6%	+20.1%
Double-Exponential	9.67×10^{-6}	7.20×10^{-5}	1.26×10^{-4}	1.43×10^{-4}	1.46×10^{-4}
(Anspaugh et al., 2002)	-85.1%	-82.1%	-75.7%	-62.8%	-58.5%
Power-Law	4.47×10^{-5}	1.06×10^{-4}	1.19×10^{-4}	1.26×10^{-4}	1.34×10^{-4}
(Maxwell and Anspaugh, 2011)	-96.8%	-87.8%	-74.2%	-57.7%	-54.8%

DISCUSSION

I. Reassessment Overview

Nearly all data extracted from the literature matched those presented in Maxwell and Anspaugh (2011). In the case of Garger (1997), data obtained spanned an additional 1000 days. One dataset (Olafson and Larson, 1961) appeared to be based on a yearly average, but was placed precariously close to deposition time.

The bin size for the regrouping of observations regression calculations possesses intrinsic constraints- at the upper end there is a risk of undersampling the faster decay process, which appears to be on the order of tens of days; at the lower end there is a risk of undersampling individual observations, resulting in an elevated importance weighting of rare occurances. The progression of finer resuspension factor predictions by the decrease of bin size will depend on the collection of additional observations in the short-term.

The two-compartment catenary model fit with σ_Y^{-2} weighting successfully predicted previous RF values to within 10-24%, and with greater regression coefficient than Maxwell and Anspaugh. The decrease in relative error in Table 2 over time accounts for an overestimation of initial resuspension and underestimation of decay constant in previous exponential models. Both NCRP and power-law models diverge at zero, requiring an artificial instantiation of applicability such an unphysical first-day constant and the lower limit of integration respectively. This renders it to have limited utility in calculating RF, especially for early exposure where these artificial fixes span 2 orders of magnitude.

II. Model recommendations

As $t_1 \rightarrow 0$ towards initial plume dispersion, $S_f(t)$ appears less appropriate for predicting RF based on the questionably high uncertainty in early resuspension. Depending on the combustion/release mechanism and resulting source term activity-size distribution, early measurements of S_f are likely to be convoluted with the competing dispersion processes; this is especially true of short-lived sources which have been observed to nucleate and coagulate at reduced rates (Stewart, 1964). Greater consistency of S_f is achieved with the activity arising from the activity size distribution characteristic to *re*suspended material available for sampling, not the initial fallout of the immediately localized plume. Early dose constructions are better suited for emergency dosimetry plans, as plume behavior greatly increases in complexity around civil structures (Eisenbud and Gesell, 1997) resulting in a widely variation in activity.

Sandia National Laboratories is a multimission laboratory managed and operated by National Technology and Engineering Solutions of Sandia, LLC., a wholly owned subsidiary of Honeywell International, Inc., for the U.S. Department of Energys National Nuclear Security Administration under contract DE-NA-0003525.

REFERENCES

A. Brodsky. Resuspension factors and probabilities of intake of material in process (or "is 10^{-6} a magic number in health physics?"). *Health Physics*, 39(6):992–1000, Dec. 1980.

NCRP. Recommended screening limits for contaminated surface soil and review of factors relevant to site-specific studies. Technical Report 129, National Council on Radiation Protection and Measurements, 1999.

R.M. Maxwell and L.R. Anspaugh. An improved model for prediction of resuspension. *Health Physics*, 101(6): 722–730, 2011.

W.H. Langham. Plutonium distribution as a problem in environmental science. *Proceedings of Environmental Plutonium Symposium*, LA-4756:3–11, 1971.

O.G. Chkhetiani, E.B. Gledzer, M.S. Artamonova, and M.A. Iordanskii. Dust resuspension under weak wind conditions: direct observations and model. *Atmospheric Chemistry and Physics*, 12:5147–5162, 2012.

M.W. Reeks, J. Reed, and D. Hall. On the resuspension of small particles by a turbulent flow. *Journal of Physics D: Applied Physics*, 21:574–589, 1988.

L.R. Anspaugh, S.L. Simon, K.I. Gordeev, I.A. Likhtarev, R.M. Maxwell, and S.M. Shinkarev. Movement of radionuclides in terrestrial ecosystems by physical processes. *Health Physics*, 82(5):669–679, 2002.

C. Henry and J-P. Minier. Progress in particle resuspension from rough surfaces by turbulent flows. *Progress in Energy and Combustion Science*, 45:1–53, 2014.

G. Ziskind, M. Fichman, and C. Gutfinger. Resuspension of particulates from surfaces to turbulent flows - review and analysis. *Journal of Aerosol Science*, 26(4):613–644, 1995.

G. Caruso, M. Nobili, and L. Ferroni. Modelling of dust resuspension in tokamak devices during an air inflow event. *Journal of Fusion Energy*, 34:1039–1050, 2015.

X. Liu, J.E. Doerges, J. Volckens, and T.E. Johnson. Aerosol size distribution in the schwarzwalder uranium mine. *Radiation Safety Journal*, 106:S20S24, 2014.

G. Lujaniene, P. Benes, K. Stamberg, and T. Sciglo. Kinetics of plutonium and americium sorption to natural clay. *Journal of Environmental Radioactivity*, 108:4149, 2012.

K. Bunzl, W. Kracke, W. Shimmack, and K. Auerswald. Migration of fallout pu-239+240, am-241 and cs-137 in the various horizons of a forest soil under pine. *Journal of Environmental Radioactivity*, 28:1734, 1995.

M.S. Lee and C.W. Lee. Association of fallout-derived cs-137, sr-90 and pu-239, pu-240 with natural organic substances in soils. *Journal of Environmental Radioactivity*, 47:25362, 2000.

A. Mori et al. The colloid and radionuclide retardation experiment at the grimsel test site: Influence of bentonite colloids on radionuclide migration in a fractured rock. *Colloid and Surfaces A*, 217:3347, 2003.

P. Vilks and D.B. Bachinski. Colloid and suspended particle migration experiments in a granite fracture. *Journal of Contaminant Hydrology*, 21:269–279, 1996.

N.D.M. Evans. Binding mechanisms of radionuclides to cement. *Cement and Concrete Research*, 38:543–553, 2008.

F. Chawla, P. Steinmann, H-R. Pfeifer, and P. Froidvaux. Atmospheric deposition and migration of artificial radionuclides in alpine soils (val pioria, switzerland) compared to distribution of selected major and trace lements. *Science of the Total Environment*, 408:3292–3302, 2010.

M. Dreicer, T.E. Hakonson, C.G. White, and F.W. Whicker. Rainsplash as a mechanism for soil contamination of plant surfaces. *Health Physics*, 46(1):177–187, 1984.

H. Muller-Lemens and F. van Dorp. Bioturbation as a mechanism for radionuclide transport in soil: Relevance of earthworms. *Journal of Envronmental Radioactivity*, 31:7–20, 1996.

G. Matisoff, M.E. Ketterer, K. Rosn, J.W. Mietelski, L.F. Vitko, H. Persson, and E. Lokas. Downward migration of chernobyl-derived radionuclides in soils in poland and sweden. *Applied Geochemistry*, 26:105–115, 2011.

E. Karlsson, I. Fangmark, and T. Berglund. Resuspension of an indoor aerosol. *Journal of Aerosol Science*, 27(Supplement 1):S441–S442, 1996.

Z. Xu, T. Jordan, and W. Breitung. Particle resuspension model for subatmospheric conditions. *IEEE Transactions on Plasma Science*, 44(9):1662–1665, 2016.

Y. Kim, G. Wellum, K. Mello, K.E. Strawhecker, R. Thoms, A. Giaya, and B.E. Wyslouzild. Effects of relative humidity and particle and surface properties on particle resuspension rates. *Aerosol Science and Technology*, 50(4): 339–352, 2016.

A.R. Harris and C.I. Davidson. Particle resuspension in turbulent flow: A stochastic model for individual soil grains. *Aerosol Science and Technology*, 42:613–628, 2008.

W.H. Langham, P.S. Harris, and T.L. Shipman. Plutonium hazards created by accidental or experimental low-order detonation of atomic weapons. Technical Report LA-1981, Los Alamos: Los Alamos National Laboratory, 1955.

J.A. Garland. Some recent studies of the resuspension of deposited material from soil and grass. *Precipitation scavaging, dry deposition, and resuspension*, pages 1087–1097, 1983.

U. Tveten. Environmental consequences of releases from nuclear accidents, a nordic perspective. Technical Report AKTU-200, Kjeller, Norway: Institute for Energy Technology, 1990.

J.A. Garland and I.R. Pomeroy. Resuspension of fall-out material following the chernobyl accident. *Journal of Aerosol Science*, 25(5):793–806, 1994.

E.K. Garger, F.O. Hoffman, K.M. Thiessen, D. Galeriu, A.I. Kryshev, T. Lev, C.W. Miller, S.K. Nair, N. Talerko, and B. Watkins. Test of existing mathematical models for atmospheric resuspension of radionuclides. *Journal of Environmental Radioactivity*, 42:157–175, 1999.

E.K. Garger, V. Kashpur, G. Belov, V. Demchuk, J. Tschiersch, F. Wagenpfeil, H.G. Paretzke, F. Besnus, W. Hollander, J. Martinez-Serrano, and I. Vintersved. Measurement of resuspended aerosol in the chernobyl area i. discussion of instrumentation and estimation of

measurement uncertainty. *Radiation Environmental Biophysics*, 1997.

J.H. Olafson and K.H. Larson. Plutonium, its biology and environmental persistence. Technical Report UCLA-501, 1961.

K. Stewart. The modes of formation and properties of aerosol particles. *Health Physics*, 10:889–897, 1964.

M. Eisenbud and T. Gesell. *Environmental Radioactivity from Natural, Industrial, and Military Sources*. San Diego, CA: Academic Press, 4 edition, 1997.